

Dynamic ^{13}N -Ammonia PET: A New Imaging Method to Diagnose Hypopituitarism

Zhang Xiangsong, MD¹; Yue Dianchao, MD²; and Tang Anwu, MD¹

¹Department of Nuclear Medicine, Guangdong Provincial People's Hospital, Guangzhou, China; and ²Department of Nuclear Medicine, The First Affiliated Hospital, Sun Yat-sen University, Guangzhou, China

We have developed a new imaging method to evaluate the blood perfusion and ammonia metabolism of the pituitary gland, and we preliminarily assessed its role in the diagnosis of hypopituitarism. **Methods:** Six female healthy volunteers (age range, 20–46 y) and 6 female patients (age range, 23–42 y) were enrolled in this study. Dynamic ^{13}N -NH₃ PET was performed. Time–activity curves for the pituitary gland and internal carotid artery were generated by setting regions of interest on the transverse planes of the pituitary gland. The standardized uptake value of the pituitary gland, the radioactive ratio of pituitary to thalamus (P/T), and the first-pass uptake rate of ammonia in the pituitary gland were calculated. **Results:** ^{13}N -Ammonia was extracted rapidly by pituitary tissue in the first 120 s after injection and trapped in pituitary tissue in the healthy volunteers. Three to 20 min after injection, the pituitary gland was clearly seen in the healthy volunteers, and the mean (\pm SD) size of the pituitary gland on ^{13}N -ammonia PET images was $(1.09 \pm 0.17 \text{ cm}) \times (1.08 \pm 0.14 \text{ cm}) \times (1.12 \pm 0.09 \text{ cm})$. However, in patients with hypopituitarism, the first-pass uptake rate of ammonia in the pituitary gland was significantly lower than that in healthy volunteers (0.35 ± 0.10 vs. 0.75 ± 0.07). On images of patients, the pituitary gland was absent or could not clearly be found, was small or malformed, and showed significantly lower uptake of ^{13}N -NH₃ than in healthy volunteers (standardized uptake value, 1.15 ± 0.34 vs. 3.74 ± 1.44 ; P/T, 0.65 ± 0.23 vs. 1.24 ± 0.34). **Conclusion:** Dynamic ^{13}N -ammonia PET can provide information on blood perfusion and metabolism of the pituitary gland and is useful in early monitoring of damage to the pituitary gland and in diagnosing hypopituitarism.

Key Words: hypopituitarism; ammonia; PET

J Nucl Med 2005; 46:44–47

The diagnosis of hypopituitarism depends mainly on symptoms and signs, the results of biochemical laboratory tests, and CT and MRI findings. However, because clinical presentation and the deficiency of pituitary hormones varies, and CT and MRI present mainly anatomic findings, early diagnosis is sometimes difficult (1).

Received Jul. 5, 2004; revision accepted Aug. 30, 2004.
For correspondence or reprints contact: Zhang Xiangsong, MD, Department of Nuclear Medicine, Guangdong Provincial People's Hospital, 106 Zhongshan Rd. II, Guangzhou 510080, China.
E-mail: sd_zh@163.net

PET is now used mainly for cancer, cardiovascular diseases, and neurologic diseases. Various tracers, such as ^{13}N -ammonia, are used in daily imaging. ^{13}N -Ammonia clears rapidly from the circulation and is taken up primarily by the myocardium, brain, liver, kidneys (2,3), and pituitary gland (4). In both myocardium and brain, ^{13}N -ammonia has been shown to be removed from the blood by single-pass extraction and to be metabolically trapped within the tissues by incorporation into the cellular pool of amino acids, mainly as glutamine (5,6).

^{13}N -Ammonia PET is rarely reported in the evaluation of endocrine disorders such as hypopituitarism. The purpose of this study was to assess the role of dynamic ^{13}N -ammonia PET in the diagnosis of hypopituitarism.

MATERIALS AND METHODS

Patients

Six female healthy volunteers (age range, 20–46 y) without pituitary disease or a history of related diseases were included as control subjects. Also included were 6 patients who had been referred to our center for evaluation of hypopituitarism diagnosed on the basis of clinical history, signs and symptoms, and biochemical tests. All patients were female, and their ages ranged from 23 to 42 y. Four had postpartum pituitary necrosis, 1 had pituitary abscess, and 1 had partial empty sella syndrome (Table 1).

The study was approved by the hospital ethics committee, and each participant gave informed consent.

PET

Dynamic PET was performed as a 3-dimensional acquisition on an ECAT HR+ scanner (Siemens/CTI) with a 5-min transmission scan. The emission protocol was a 20-min dynamic scan ($10 \text{ s} \times 12$, $30 \text{ s} \times 6$, and $900 \text{ s} \times 1$) triggered simultaneously with a bolus injection of 444–592 MBq of ^{13}N -ammonia.

Data Analysis

Regions of interest for the pituitary gland and internal carotid artery were set on the transaxial plane of the pituitary gland. We calculated the standardized uptake value of the pituitary gland, the radioactive ratio of pituitary to thalamus (P/T), and the first-pass uptake rate of ammonia in the pituitary gland, which was the radioactive ratio of pituitary to internal carotid artery in the transaxial plane of the dynamic PET frame showing the highest radioactivity in the internal carotid artery. Time–activity curves for the pituitary gland and internal carotid artery were generated.

TABLE 1
Results of Biochemical Tests on Patients with Hypopituitarism

Test	Patient 1	Patient 2	Patient 3	Patient 4	Patient 5	Patient 6	Reference value
Thyroid-stimulating hormone	0.61	0.17	0.36	0.33	0.31	0.25	0.34–5.6 mIU/L
Free thyroxine index	1.77	4.44	1.14	2.86	0.97	1.68	12.0–22.0 pmol/L
Free triiodothyronine index	3.63	3.25	1.72	3.05	2.55	1.92	3.95–6.80 pmol/L
Follicle-stimulating hormone	2.93	1.11	1.63	1.76	3.23	5.31	16.7–113.5 IU/L
Luteinizing hormone	1.22	0.42	0.36	0.92	2.50	4.63	10.8–58.6 IU/L
Prolactin	5.41	35.59	2.82	4.91	9.34	117.00	15.18–121.36 pmol/L
Adrenocorticotrophic hormone	6.7	7.9	1.36	7.7	4.25	5.13	2.64–8.16 pmol/L
Growth hormone		<4.65	9.3	7.44	4.65	8.37	0.93–51.16 pmol/L

RESULTS

^{13}N -Ammonia was extracted rapidly by pituitary tissue in a healthy volunteer (Fig. 1A); however, the pituitary gland was not apparent in a patient with Sheehan's syndrome (Fig. 1B) in first 120 s after injection. On PET images 6 min after injection, the pituitary gland was clearly seen, with high uptake of ^{13}N -ammonia, in the healthy volunteer (Fig. 2A) but was smaller, with significantly decreased uptake of ^{13}N -ammonia, in the patient with Sheehan's syndrome (Fig. 2B). Figure 3 shows typical time–activity curves, obtained from dynamic ^{13}N -ammonia PET, for the pituitary gland and internal carotid artery of a healthy volunteer and a patient with hypopituitarism.

Table 2 shows the results of dynamic ^{13}N -ammonia PET for the control group and the patient group. The first-pass uptake rate of ammonia in the pituitary gland was significantly lower in patients with hypopituitarism than in healthy volunteers (0.35 ± 0.10 vs. 0.75 ± 0.07). Three to 20 min after injection, the pituitary gland was clearly evident in the healthy volunteers, and the mean (\pm SD) size of the pituitary gland in ^{13}N -ammonia PET images was $(1.09 \pm 0.17 \text{ cm}) \times (1.08 \pm 0.14 \text{ cm}) \times (1.12 \pm 0.09 \text{ cm})$. However, the pituitary gland was absent or not clearly seen in 2 patients with Sheehan's syndrome, small in another 2 patients with Sheehan's syndrome and 1 patient with partial empty sella syndrome, and malformed in 1 patient with pituitary abscess, and uptake of ^{13}N -NH₃ in the pituitary gland was significantly lower in patients

with hypopituitarism than in healthy volunteers (standardized uptake value, 1.15 ± 0.34 vs. 3.74 ± 1.44 ; P/T, 0.65 ± 0.23 vs. 1.24 ± 0.34).

DISCUSSION

Hypopituitarism can be caused by tumors of the pituitary gland, hypothalamus, or brain; by head trauma, radiation, or surgery; by postpartum pituitary necrosis (Sheehan's syndrome); or by infection or inflammation. Clinical presentation varies. In general, more than 75% of the anterior pituitary tissue must be destroyed to produce symptoms of hormone deficiency. The low level of pituitary hormones can also vary. Usually, the deficiency of luteinizing hormone, follicle-stimulating hormone, and prolactin appears earlier and is more significant than the deficiency of thyroid-stimulating hormone and adrenocorticotrophic hormone. Hypopituitarism is difficult to diagnose in the early stage.

Sheehan's syndrome is a pituitary necrosis after postpartum hemorrhaging and hypovolemia. It usually is diagnosed retrospectively, sometimes after a delay of several years, as a classic cause of hypopituitarism (7), and few cases have been diagnosed during the acute phase. With improvements of obstetric care, Sheehan's syndrome is decreasing in frequency and hypophysitis has become the most common cause of postpartum hypopituitarism. Although the diagnosis of an empty sella has no clinical consequences, the early diagnosis of Sheehan's syndrome may be important to

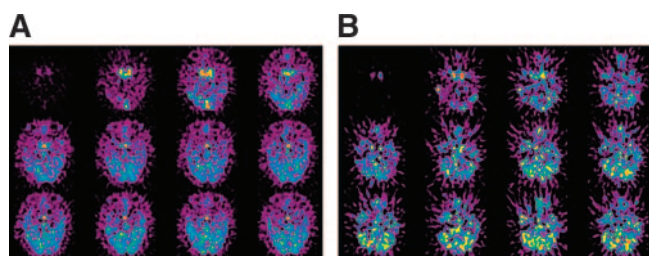


FIGURE 1. Transaxial planes of pituitary gland on dynamic ^{13}N -ammonia PET (10 s/frame). (A) Pituitary gland (arrow) was visible 10 s after internal carotid artery became evident in healthy volunteer. (B) Pituitary gland was not visible 120 s after internal carotid artery became evident in patient with Sheehan's syndrome.

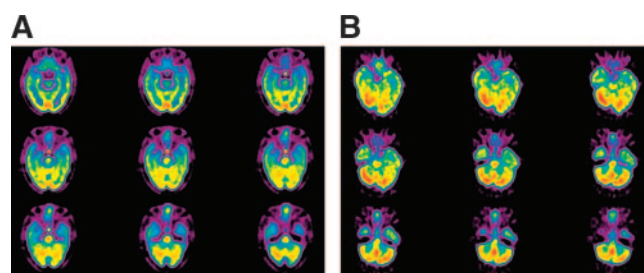


FIGURE 2. Transaxial planes of pituitary gland on ^{13}N -ammonia PET images 6 min after injection. (A) Pituitary gland was clearly evident in healthy volunteer. (B) Pituitary gland was smaller, and uptake of ^{13}N -ammonia significantly decreased, in patient with Sheehan's syndrome.

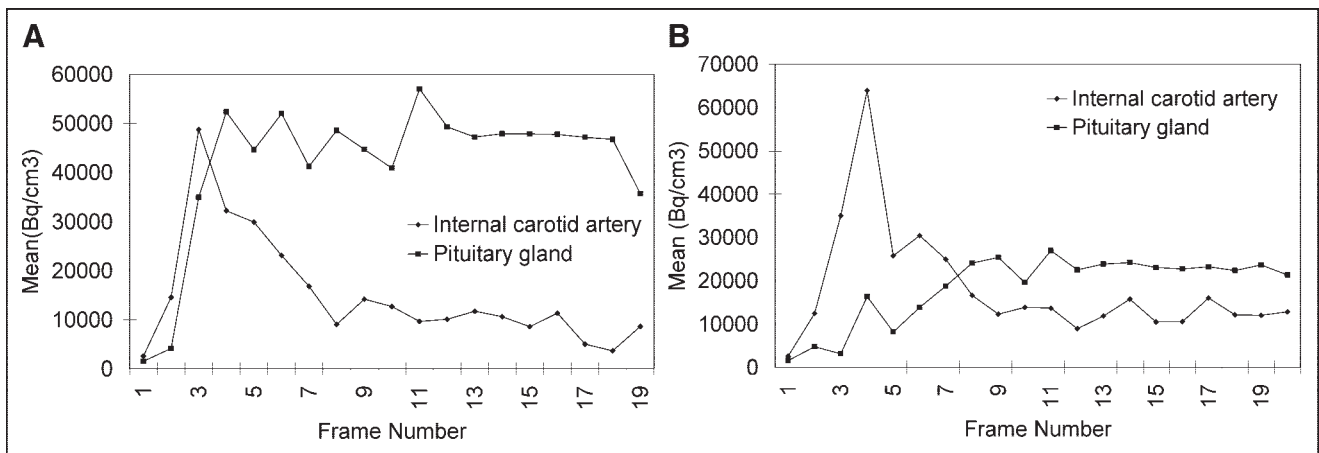


FIGURE 3. Time-activity curves, obtained from dynamic ^{13}N -ammonia PET, for pituitary gland and internal carotid artery of healthy volunteer (A) and patient with hypopituitarism (B).

establish the best therapeutic approach. In the acute phase, Sheehan's syndrome may present as an enlarged pituitary gland, which is difficult to differentiate from lymphocytic hypophysitis or pituitary adenoma, but the differential diagnosis is important for the best therapeutic management (8).

The findings of the current study suggest several similarities in the uptake and retention of ^{13}N -ammonia in the pituitary gland, brain, and myocardium. Metabolic trapping of ^{13}N -ammonia in brain and myocardium occurs primarily via the glutamate-glutamine pathway (9,10). In 1999, Shirasawa (9) detected expression of glutamine synthetase in the folliculostellate cells of the anterior pituitary gland of rats. The physiologic function of fol-

liculostellate cells is still unclear. They are postulated to be an important source of factors, such as follistatin, that regulate pituitary function by intercellular communication. By maintaining an optimal concentration of amine and glutamic acid, one can modulate the excretion of pituitary hormones (11). One can speculate that the glutamate-glutamine pathway is the primary mechanism of ^{13}N -ammonia metabolism in the pituitary gland.

^{13}N -Ammonia has been proved to be a good indicator of myocardial blood flow and a reflection of metabolic integrity (12,13). The time-activity curves for pituitary tissue and myocardium are quite similar. Therefore, one can speculate that the kinetics of ^{13}N -ammonia in pituitary gland and myocardium are similar and that ^{13}N -ammonia is a good

TABLE 2
 ^{13}N -Ammonia PET Findings in Healthy Volunteers and Patients with Hypopituitarism

Subject no.	Age (y)	Sex	Dimensions (cm)	R	SUV	P/T
Volunteer						
1	20	F	1.13 × 1.14 × 1.14	0.81	4.25	1.23
2	25	F	0.93 × 1.03 × 1.03	0.70	3.67	1.07
3	46	F	1.03 × 1.02 × 1.13	0.76	1.73	0.96
4	38	F	0.91 × 0.93 × 1.01	0.67	5.68	1.91
5	42	F	1.34 × 1.33 × 1.24	0.72	2.48	1.18
6	35	F	1.24 × 1.03 × 1.15	0.85	4.62	1.11
Mean			1.09 × 1.08 × 1.12	0.75	3.74	1.24
SD			0.17 × 0.14 × 0.09	0.07	1.44	0.34
Patient						
1	23	F	0.82 × 0.83 × 0.82	0.35	1.53	0.79
2	33	F	(No uptake)	0.27	0.83	0.43
3	35	F	(No uptake)	0.21	0.67	0.30
4	42	F	0.72 × 0.85 × 0.79	0.38	1.12	0.69
5	28	F	0.91 × 1.18 × 1.25	0.45	1.29	0.82
6	39	F	0.85 × 0.88 × 0.91	0.47	1.43	0.88
Mean				0.35	1.15	0.65
SD				0.10	0.34	0.23
P				0.0001	0.002	0.006

SUV = standardized uptake value.

indicator of pituitary blood flow and a reflection of the metabolic integrity of pituitary tissue.

In this study we found that, compared with healthy volunteers, patients with hypopituitarism showed significantly decreased ^{13}N -ammonia uptake, suggesting a decreased blood supply or deficiency of the expressed activity of glutamine synthetase in folliculostellate cells.

CONCLUSION

Dynamic ^{13}N -ammonia PET can provide information on the blood perfusion and metabolism of the pituitary gland—information that will complement the anatomic details provided by CT and MRI and be useful in early monitoring of damage to the pituitary gland and in differentiating the causes of hypopituitarism.

ACKNOWLEDGMENTS

This work was partially supported by grant A2003039 from the Medical Sciences Foundation of Guangdong Province, China, and grant 031652 from the Nature Sciences Foundation of Guangdong Province, China.

REFERENCES

1. Schmidt DN, Wallace K. How to diagnose hypopituitarism: learning the features of secondary hormonal deficiencies. *Postgrad Med.* 1998;104:77–87.
2. Hunter WW, Monahan WG. A new physiological radiotracer for molecular medicine [abstract]. *J Nucl Med.* 1971;12:368.
3. Monahan WG, Tilbury RS, Laughlin JS. Uptake of ^{13}N -labeled ammonia. *J Nucl Med.* 1972;13:274–277.
4. Zhang XS, Tang AW, Qiao SX, et al. The preliminary study of the blood perfusion and ammonia metabolism of pituitary using dynamic ^{13}N - NH_3 PET imaging. *Chinese J Nucl Med.* 2002;22:141–142.
5. Harper PV, Lathrop KA, Krizek H, et al. Clinical feasibility of myocardial imaging with ^{13}N , *J Nucl Med.* 1972;13:278–280.
6. Phelps ME, Hoffman EJ, Coleman RE, et al. Tomographic images of blood pool and perfusion in brain and heart. *J Nucl Med.* 1976;17:603–612.
7. Vance ML. Hypopituitarism. *N Engl J Med.* 1994;330:1651–1652.
8. Dejager S, Gerber S, Foubert L, Turpin G. Sheehan's syndrome: differential diagnosis in the acute phase. *J Intern Med.* 1998;244:261–266.
9. Shirasawa N, Yamanouchi H. Glucocorticoids induce glutamine synthetase in folliculostellate cells of rat pituitary glands in vivo and in vitro. *J Anat.* 1999;194:567–577.
10. Schelbert HR, Phelps ME. Physiologic tomography: a new means for the non-invasive measurement of myocardial metabolism, blood flow and function. *Eur J Nucl Med.* 1980;5:209–215.
11. Cooper AJL, McDonald JM, Gelbard AS, et al. The metabolic fate of ^{13}N -labeled ammonia in rat brain. *J Biol Chem.* 1979;254:4982–4992.
12. Schelbert HR, Phelps ME, Huang SC, et al. N-13 ammonia as an indicator of myocardial blood flow. *Circulation.* 1981;63:1259–1272.
13. Henze E, Schelbert HR, Barrio JR, et al. Evaluation of myocardial metabolism, with N-13- and C-11-labeled amino acids and positron computed tomography. *J Nucl Med.* 1982;23:671–681.

